Paper 264

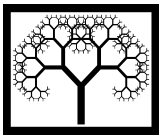

Proceedings of the Eleventh International Conference
on Computational Structures Technology,
B.H.V. Topping, (Editor),
Civil-Comp Press, Stirlingshire, Scotland

Calibration of a Distortional Hardening Model of Plasticity

J. Plešek[1], Z. Hrubý[1], S. Parma[1], H.P. Feigenbaum[2] and Y.F. Dafalias[3]
[1] Institute of Thermomechanics
Academy of Sciences of the Czech Republic, Prague
[2] Department of Mechanical Engineering
Northern Arizona University, Flagstaff, USA
[3] Department of Civil and Environmental Engineering
University of California at Davis, USA

Abstract

Directional distortion hardening is manifested by the distortion of the shape of the yield surface such that a region of high curvature develops roughly in the direction of loading while a region of lower curvature develops in the opposite direction. Recently, several models were proposed. The simplest one studied, makes use of the Armstrong-Frederick rule, having five independent parameters. The analytical solution for uniaxial cyclic test is derived together with that for the stabilized cyclic response. The evolving shapes of the yield surfaces and their sensitivity to inputs parameters are analysed. An algorithm for material constants fitting is proposed.

Keywords: directional distortional hardening, metal plasticity, yield surface.

1 Introduction

Distortion of yield surfaces due to strain hardening was observed in numerous experiments with various types of metals [1, 2]. In stress space, the subsequent yield surfaces assume egg shape contours, being highly curved in the direction of loading and flattened in the opposite direction. Following several attempts at modelling such behaviour in the past, three promising approaches have been proposed recently. Feigenbaum and Dafalias developed the celebrated Armstrong-Frederick idea [3] into constructing directional terms involving the inner product of the backstress with local normal tensors, giving rise to two model concepts: *i*) one [4] utilizing fourth order evolution tensor and *ii*) the other [5] with fixed directional support (discussed in this paper). One may add to that even more general proposition by Shutov et al. [6], when *iii*) a sixth order anisotropy tensor was used to the same end.

The usual problem arises with the identification of all the necessary parameters for evolving internal tensorial variables. Apart from thermodynamic constraints derived

in the original papers by Feigenbaum and Dafalias [4, 5], conditions on maintaining convexity of distorted surfaces should be met, as noted by Plesek et al. [7], so that the convergence of return mapping numerical integrators was guaranteed [8]. Despite the undisputable potential of simple trial and error fitting methods introduced in reference [9] to systematically analyze essential features of the proposed models, there has still been a call for lucid material constants calibration. Indeed, in practice, the availability of such procedures is often a decisive factor in engineering preferences regarding the choice of a constitutive model.

It turns out that even for the simplest loading modes, such as the uniaxial stress state or pure shear, the reduced algebro-differential systems corresponding to majority of distortional hardening models are excessively complex not permitting analytical solutions. This, of course, hinders finding a proper way to identify material parameters from tensile or torsion tests. The present paper, nevertheless, shows that at least for one of the models mentioned a close form solution exists and may be used for calibration purposes. The knowledge of such solution may also lend some help in more complex cases, supplying first approximation as well as general guidlines.

This text is organized as follows. The next section overviews the so called c-model, the simplest of the family, including examples of evolving yield surfaces and hardening curves. In Section 3, analytical solutions for fundamental loading cases are provided, followed by the proposal of the set of algebraic equations suitable for constants identification. Before concluding, sensitivity of the model's response to variation of input parameters is studied.

2 Constitutive model overview

Initially, the yield function f takes on a character of the J_2-invariant, which is subsequently modified by evolving multiplier as

$$f(\boldsymbol{\sigma}) = \frac{3}{2}\left[1 - c(\mathbf{n}_r : \boldsymbol{\alpha})\right] \|\mathbf{s} - \boldsymbol{\alpha})\|^2 - k^2 \leq 0 \tag{1}$$

Here $\boldsymbol{\sigma}$ is the stress tensor; $\mathbf{s}$ deviatoric stress; $\boldsymbol{\alpha}$ is the backstress; c is a positive material constant; k is a scalar internal variable; the double dot symbol represents the inner product of two tensors as in $\mathbf{s} : \boldsymbol{\alpha} = s_{ij}\alpha_{ij}$ and $\|\cdot\|$ denotes the Euclidean norm of a second order tensor. Finally,

$$\mathbf{n}_r := \frac{\mathbf{s} - \boldsymbol{\alpha}}{\|\mathbf{s} - \boldsymbol{\alpha}\|} \tag{2}$$

is the unit tensor pointing in the direction of loading relative to the centroid of the yield surface. Hence, it is the inner product $\mathbf{n}_r : \boldsymbol{\alpha}$ which forms the shape of the yield surface.

The model's internal variables are governed by the standard evolution equations. Plastic strain obeys the associated flow rule

$$\dot{\boldsymbol{\epsilon}}^p = \lambda \frac{\partial f}{\partial \boldsymbol{\sigma}} \tag{3}$$

the kinematic hardening rule of Armstrong-Frederick's type retains the evanescent memory member so that

$$\dot{\boldsymbol{\alpha}} = a_1(\dot{\boldsymbol{\epsilon}}^p - a_2\|\dot{\boldsymbol{\epsilon}}^p\|\boldsymbol{\alpha}) \tag{4}$$

and similarly for the kinematic part

$$\dot{k} = \lambda\kappa_1 k(1 - \kappa_2 k) \tag{5}$$

The initial values at time $t = 0$ are defined as $\boldsymbol{\epsilon}^p = \mathbf{0}$, $\boldsymbol{\alpha} = \mathbf{0}$ and $k = k_0$, that is, k_0 is the initial yield stress. Details of this constitutive model, which features six positive constants, a_1, a_2, κ_1, κ_2, k_0, and c are explained in reference [5].

Before proceeding further on, it is useful to have some formulas ready. One may explicitly calculate the gradient

$$\frac{\partial f}{\partial \boldsymbol{\sigma}} = \frac{3}{2}\|\mathbf{s} - \boldsymbol{\alpha}\|[2\mathbf{n}_r - c(\mathbf{n}_r : \boldsymbol{\alpha})\mathbf{n}_r - c\boldsymbol{\alpha}] \tag{6}$$

and its magnitude as

$$\left\|\frac{\partial f}{\partial \boldsymbol{\sigma}}\right\| = \frac{3}{2}\|\mathbf{s} - \boldsymbol{\alpha}\|\sqrt{[2 - c(\mathbf{n}_r : \boldsymbol{\alpha})][2 - 3c(\mathbf{n}_r : \boldsymbol{\alpha})] + c^2\boldsymbol{\alpha} : \boldsymbol{\alpha}} \tag{7}$$

Moreover

$$\frac{\partial f}{\partial \boldsymbol{\sigma}} = \left\|\frac{\partial f}{\partial \boldsymbol{\sigma}}\right\|\mathbf{n} \tag{8}$$

where $\mathbf{n}$ is the outward unit normal to the yield surface.

It was proved by these authors in references [5, 7] that the necessary and sufficient condition, which renders dissipation positive and, simultaneously, preserves strict convexity for all times, reads

$$\|c\boldsymbol{\alpha}\| < 1 \tag{9}$$

Working on that condition, one may insert Equation (8) into the flow rule and then into Equation (4) to obtain

$$\dot{\boldsymbol{\alpha}} = a_1\lambda\left\|\frac{\partial f}{\partial \boldsymbol{\sigma}}\right\|(\mathbf{n} - a_2\boldsymbol{\alpha}) \tag{10}$$

For monotonic loading and as $t \to \infty$ the saturated state is reached when

$$\mathbf{n} - a_2\boldsymbol{\alpha} = \mathbf{0} \tag{11}$$

Since $\boldsymbol{\alpha}$ starts from zero and the magnitude of the limit backstress, $1/a_2$, is independent of the loading direction, we may write

$$\|\boldsymbol{\alpha}\| \leq 1/a_2 \tag{12}$$

Hence the left-hand side of Inequality (9) may be bounded by c/a_2, which yields

$$c < a_2 \tag{13}$$

This is the only constraint to be observed in constitutive modelling.

2.1 Sample illustration

To illustrate the behaviour of the discussed model let us employ the same values of material parameters as in reference [5]. Thus, $a_1 = 10500$ MPa, $a_2 = 0.02$ MPa^{-1}, $\kappa_1 = 6000$ MPa, $\kappa_2 = 0.012$ MPa^{-1}, $c = 0.019$ MPa^{-1}, $k_0 = 128$ MPa. Note, that the condition stipulated by Inequality (13) is fulfilled.

Material is first loaded by uniaxial tension until the limit state has been reached. Figure 1 shows the evolution of subsequent yield surfaces as perceived in two subspaces. Likewise, the material may be loaded by prescribed strain. Evolution of the strain driven loci is similar and is not shown.

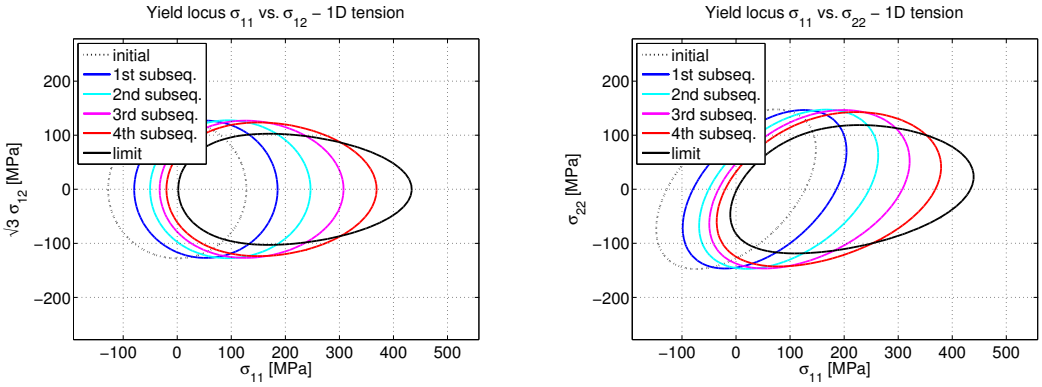

Figure 1: Yield loci evolution for stress driven loading

It is also worth studying stress-strain curves and the distribution of other internal variables. This is plotted in Figure 2 both for stress and strain driven loadings.

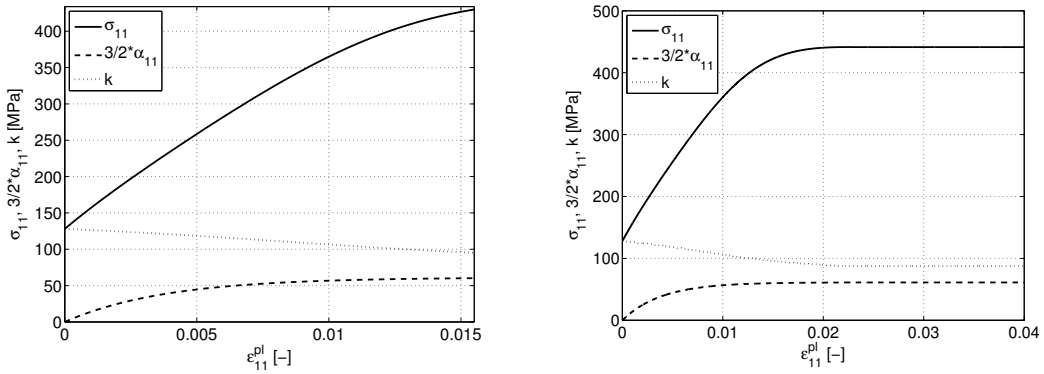

Figure 2: Variables distribution for stress (left) and strain driven (right) loadings

3 Simple loading modes

Before any attempt at the determination of material constant can be made, analytical solutions to typical loading cases, which occur in experimental arrangements, must

be found. In this section the uniaxial state of stress is discussed, which is important for tension-compression tests. Unfortunately, neither pure shear nor any other proportional load brings about new information since the ensuing equations are mere multiples of one another.

For those reasons, we turn our attention to stabilized cyclic deformation curves, which may be extracted from the model's governing equations. One disadvantage of this approach is that the two problems, i.e. evolution versus cyclicly stabilized response, are not fully compatible, the latter containing only certain material constants. Nevertheless, a suitable combination of both may provide a sufficient number of equations to calibrate our model.

3.1 Uniaxial stress

In the tensile test all components of the stress tensor, except σ_{11}, are zero. The yield condition, Equation (1), then becomes

$$f(\boldsymbol{\sigma}) = \frac{9}{4}(s_{11} - \alpha_{11})^2(1 - \sqrt{\frac{3}{2}}\,\mathrm{sgn}\, c\alpha_{11}) - k^2 \leq 0 \tag{14}$$

where the symbol ' sgn ' stands for the sign of $(s_{11} - \alpha_{11})$, that is

$$\mathrm{sgn}\ := \frac{s_{11} - \alpha_{11}}{|s_{11} - \alpha_{11}|} \tag{15}$$

Note, that $\|\boldsymbol{\alpha}\| = \sqrt{3/2}|\alpha_{11}|$, which together with Inequalities (12) and (13) implies

$$1 - \sqrt{\frac{3}{2}}\,\mathrm{sgn}\, c\alpha_{11} \geq 1 - \frac{c}{a_2} > 0 \tag{16}$$

This, very important relation, not only renders f meaningful but also applies to other expressions that will follow. Using the previous results, Equation (6) and (7) one obtains

$$\frac{\partial f}{\partial \sigma_{11}} = 3(s_{11} - \alpha_{11})(1 - \sqrt{\frac{3}{2}}\,\mathrm{sgn}\, c\alpha_{11}) \tag{17}$$

and

$$\left\| \frac{\partial f}{\partial \sigma_{11}} \right\| = 3\sqrt{\frac{3}{2}}|s_{11} - \alpha_{11}|(1 - \sqrt{\frac{3}{2}}\,\mathrm{sgn}\, c\alpha_{11}) \tag{18}$$

Because of property (16), absolute value does not need to be used for the bracketed term.

At this point, all the remaining evolution equations may be specified. The flow rule reduces to

$$\dot{\epsilon}^p_{11} = 3\lambda(s_{11} - \alpha_{11})(1 - \sqrt{\frac{3}{2}}\,\mathrm{sgn}\, c\alpha_{11}) \tag{19}$$

the backstress

$$\dot{\alpha}_{11} = a_1(1 - \sqrt{\frac{3}{2}}\,\mathrm{sgn}\, a_2\alpha_{11})\dot{\epsilon}^p_{11} \tag{20}$$

and the isotropic variable

$$\dot{k} = \lambda \kappa_1 k (1 - \kappa_2 k) \tag{21}$$

which completes an ordinary differential system.

It is easy to integrate the stand alone Equation (20) even for cyclic loading with possible stress reversals. This results in

$$\alpha_{11} = \sqrt{\frac{2}{3}} \frac{\operatorname{sgn}}{a_2} \left[1 - (1 - \sqrt{\frac{3}{2}} \operatorname{sgn} a_2 \alpha_{11}^0) \exp\left(-\sqrt{\frac{2}{3}} \operatorname{sgn} a_1 a_2 \Delta \epsilon_{11}^p \right) \right] \tag{22}$$

where α_{11}^0 denotes the value, which the backstress component attained at the end of the previous loading cycle, and $\Delta \epsilon_{11}^p$ is the increment of plastic strain in the current cycle. For example, in the first tensile quarter-cycle one has

$$\alpha_{11} = \sqrt{\frac{2}{3}} \frac{1}{a_2} \left[1 - \exp\left(-\sqrt{\frac{2}{3}} a_1 a_2 \Delta \epsilon_{11}^p \right) \right] \tag{23}$$

etc.

Next, we eliminate λ from Equation (19), substitute into Equation (21) and with the aid of Equation (14) arrive at

$$\frac{2\dot{k}}{\kappa_1 (1 - \kappa_2 k)} = \frac{\operatorname{sgn} \dot{\epsilon}_{11}^p}{\sqrt{1 - c\sqrt{\frac{3}{2}} \operatorname{sgn} \alpha_{11}}} \tag{24}$$

This differential equation may look chalenging at first glance but even in this case a series of substitutions leads to a desirable, though rather complex result

$$k = \frac{1}{\kappa_2} [1 - (1 - \kappa_2 k_0) \exp(\xi)] \tag{25}$$

where

$$\xi = -\sqrt{\frac{2}{3}} \frac{\kappa_1 \kappa_2}{a_1 \sqrt{a_2 (a_2 - c)}} (\tanh^{-1}(p) - \tanh^{-1}(p_0)) \tag{26}$$

and

$$p(\Delta \epsilon_{11}^p) = \sqrt{1 + \frac{c}{a_2 - c} \left(1 - \sqrt{\frac{3}{2}} \operatorname{sgn} a_2 \alpha_{11}^0 \right) \exp\left(-\sqrt{\frac{3}{2}} \operatorname{sgn} a_1 a_2 \Delta \epsilon_{11}^p \right)} \tag{27}$$

with $p_0 = p(0)$. Assuming plastic yielding, Equation (14) must be satisfied with the '=' sign, which gives

$$\sigma_{11} = \frac{\operatorname{sgn} k}{\sqrt{1 - \sqrt{\frac{3}{2}} \operatorname{sgn} c \alpha_{11}}} + \frac{3}{2} \alpha_{11} \tag{28}$$

Substituting for α_{11} and k, the closed form solution is obtained.

As was already mentioned in the introduction to this section, equivalent systems hold for other proportional loading paths so that no extra information can be gained in this fashion and alternatives should be sought.

3.2 Stabilized hysteresis loop

Suppose that the material is cyclicaly loaded with constant plastic deformation $\pm\hat{\epsilon}^p$. Once the saturated state has been reached, the isotropic part of hardening ceases to evolve. Basically, the state of saturation may be modelled as a combination of kinematic and distortional portions of hardening—see Figure 3—with k fixed to its limit value $1/\kappa_2$. Moreover, one may safely assume that stress oscillations will also stabilize to $\pm\hat{\sigma}$. The curve connecting the apices of limit hysteresis loops, corresponding to different amplitudes, defines the cyclic deformation curve.

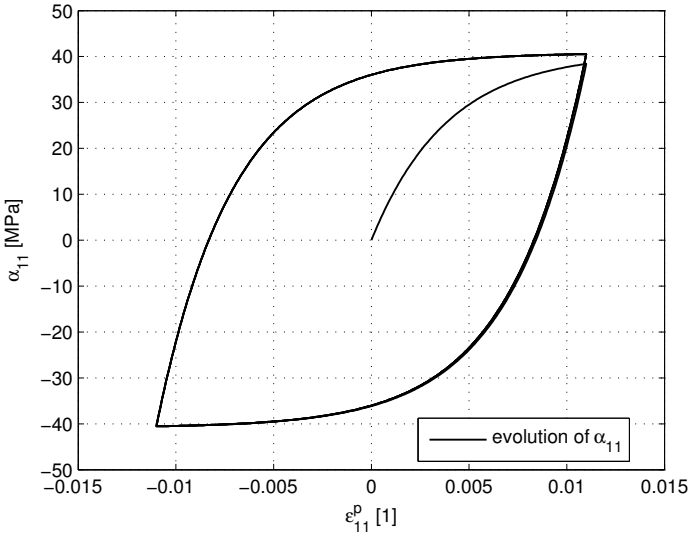

Figure 3: Stabilized backstress response

According to Lemaitre and Chaboche [10], possibly the simplest way to obtain a formula for the cyclic curve is to make an assumption that the backstress hysteresis given by Equation (22) has to create a closed loop. Hence

$$\hat{\alpha} = \sqrt{\frac{2}{3}}\frac{1}{a_2}\left[1 - (1 + \sqrt{\frac{3}{2}}a_2\hat{\alpha})\exp\left(-2\sqrt{\frac{2}{3}}a_1a_2\hat{\epsilon}^p\right)\right] \tag{29}$$

where we have substituted $\alpha_{11} = \pm\hat{\alpha}$. From Equation (29) one immediately gets

$$\hat{\alpha} = \sqrt{\frac{2}{3}}\frac{1}{a_2}\tanh\left(\sqrt{\frac{3}{2}}a_1a_2\hat{\epsilon}^p\right) \tag{30}$$

Making use of Equation (14), the stress-strain curve takes the form

$$\hat{\sigma}(\hat{\epsilon}^p) = \frac{1}{\kappa_2\sqrt{1 - \dfrac{c}{a_2}\tanh\left(\sqrt{\dfrac{3}{2}}a_1a_2\hat{\epsilon}^p\right)}} + \sqrt{\frac{3}{2}}\frac{1}{a_2}\tanh\left(\sqrt{\frac{3}{2}}a_1a_2\hat{\epsilon}^p\right) \tag{31}$$

It should be pointed out that the cyclic yield stress defined in the limit as $\hat{\epsilon}^p \to 0$ amounts to $\hat{k}_0 = 1/\kappa_2$, which differs from k_0. Incidentally, $1/\kappa_2$ is the limit value of k. For example, for the material in question $\hat{k}_0 = 83$ MPa as opposed to $k_0 = 128$ MPa, indicating cyclic softening. This may also be seen in Figure 2, where the isotropic variable indeed decreases.

4 Calibration

Assuming that the initial yield tress, k_0, is known, there are five material constants to be determined. In principle, Equation (28) by itself is sufficient since it contains all the free parameters. One may think, for instance, of fitting it against several points selected on the loading-unloading branches of an experimental stress-strain curve. Such a simplistic approach, nevertheless, does not need to be necessarily expedient, therefore, one may look for alternatives.

Sensitivity analysis, presented in the next section, suggests that the constant κ_2 does not strongly influence transient evolution, therefore, its value may be readily obtained as the reciprocal of the cyclic yield stress $\hat{k}_0$. This reduces the number of unknowns to four. Asymptotics to Equation (31) as $\hat{\epsilon}^p \to \infty$ provides us with another clue

$$\hat{\sigma}_\infty = \frac{\hat{k}_0}{\sqrt{1 - \dfrac{c}{a_2}}} + \sqrt{\frac{3}{2}}\frac{1}{a_2} \tag{32}$$

Thus, combining Equations (28), (31) and (32) one can set up a nonlinear algebraic system consisting of a sufficient number of equations to be solved for a_1, a_2, κ_1 and c.

4.1 Sensitivity analysis

A revealing insight into the process of calibration may be gained by sensitivity analysis. In this work, such analysis was carried out numerically, varying each input parameter, one at a time, by adding or subtracting fifty per cent of its nominal value. The results are shown in Figures 4-8

It follows from the plots of yield loci that the constitutive model enjoys considerable stability with respect to input variation. It seems that apart from the yield stress k_0, the most influential constant is the parameter c that controls directional distortional hardening.

5 Conclusions

One of the recently proposed constitutive models with directional distortional hardening was studied in detail. This model, suitable for metal plasticity, represents probably

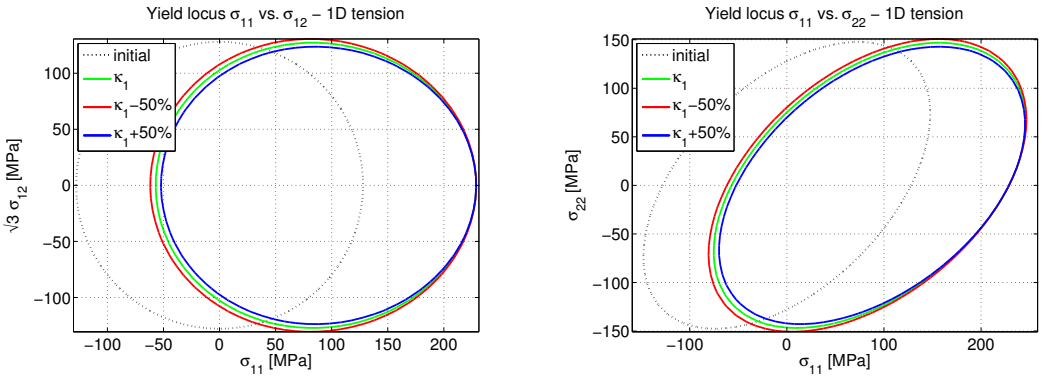

Figure 4: Sensitivity to κ_1

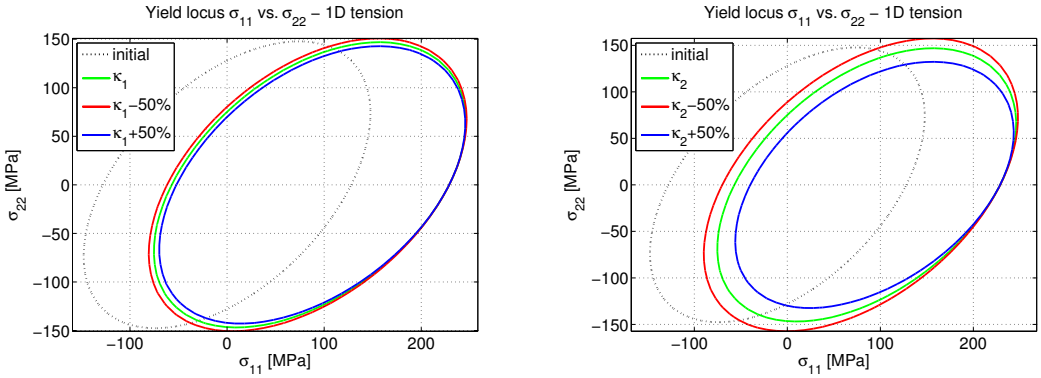

Figure 5: Sensitivity to κ_2

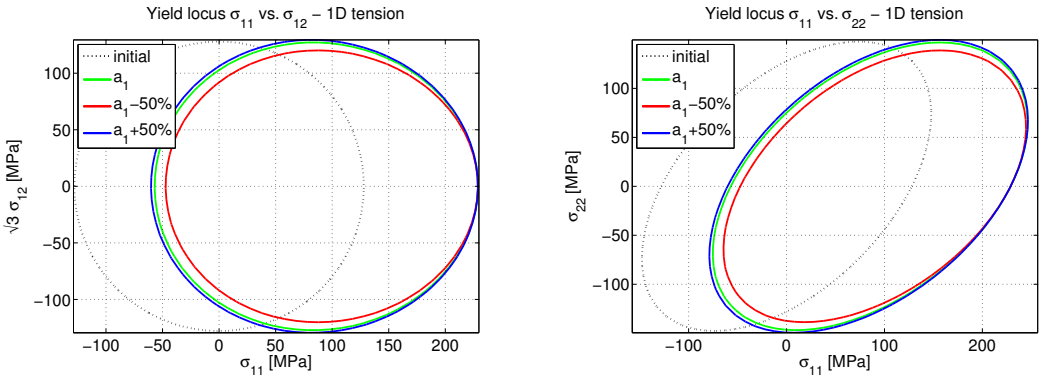

Figure 6: Sensitivity to a_1

the simplest conceivable form of constitutive equations that, not counting elastic constants and the initial yield stress, list only five additional material parameters. Despite of seeming simplicity, this model can capture reasonably well all the essential features of a yield surface distortion. Four of the constants enter the Armstrong-Frederick type evolution equations with recall memory terms for backstress and the isotropic variable. The fifth parameter controls directional multiplier, which, motivated by the AF rule, consists of the inner product of the stress tensor with backstress.

A major problem, quite common with many complex plasticity models, arises when

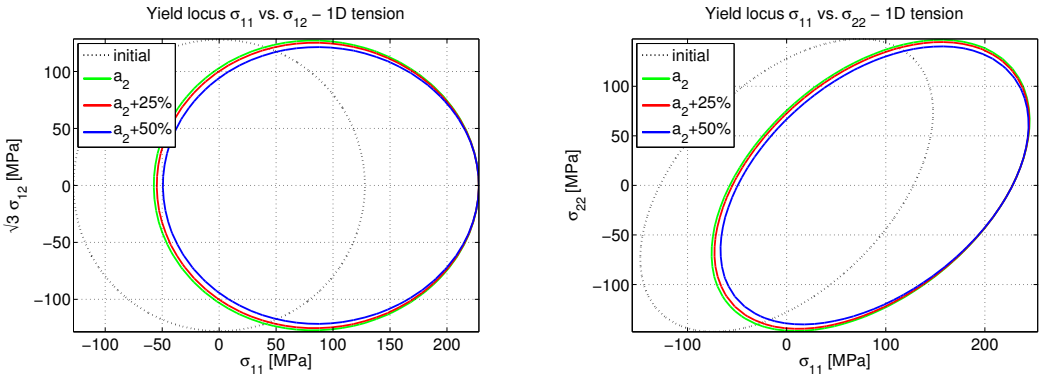

Figure 7: Sensitivity to a_2

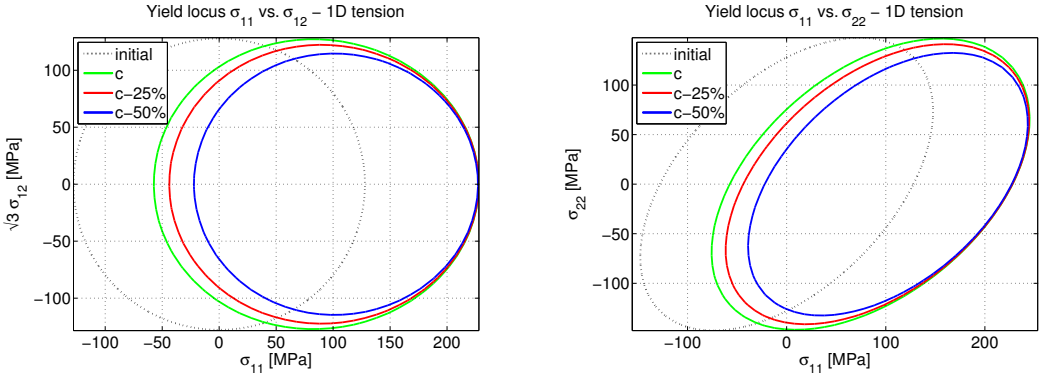

Figure 8: Sensitivity to c

a user wishes to identify material parameters for a particular application. Reduction of constitutive equations to one variable form characteristic of uniaxial stress, as in the tensile test, or pure shear, as in the torsion test, leads to an algebro-differential system difficult (if not impossible) to solve. For the problem at hand, s solution is feasible yet it gives rise to a set of nonlinear algebraic equations, which must be dealt with numerically.

The idea of computing asymptotic states for cyclically loaded specimens may lend some help. Indeed, the ensuing equations are much simpler, nonetheless, not fully compatible with the ones describing transient evolution close to the initial state. For example, the cyclic yield stress conforming to small plastic strain amplitude does not equal the monotonic yield stress, which is usually significantly larger. Accepting some shortcomings, monotonic and cyclic loading curves, if available, provide a sufficient data set for the material model calibration.

The last section outlined a promising method, based on sensitivity analysis, to select the optimum loading modes, which are best suited for tuning certain model parameters. Although numerical by nature, this investigation unveiled low sensitivity of the yield surface morphology to most constants except for the ones controlling directional distortional hardening and the ultimate yield strength.

Acknowledgements

This work was supported by GACR 101/09/1630 and GACR P201/10/0357 granted projects in the framework of AV0Z20760514 research plan.

References

[1] H.C. Wu, W. Yeh, "On the experimental determination of yield and some results of annealed 304 stainless steel", Int. J. Plasticity, 7, 803-826, 1991.

[2] M. Boucher, P. Cayla, J.P. Cordebois, "Experimental studies of yield surfaces of aluminum alloy and low carbon steel under complex biaxial loadings", Eur. J. Mech. Solids/A, 14, 1-17, 1995.

[3] P.J. Armstrong, C.O. Frederick, C.O., "A mathematical representation of the multiaxial Bauschinger effect", CEGB Report, RD/B/N731, 1966.

[4] H.P. Feigenbaum, Y.F. Dafalias, "Directional distortional hardening in metal plasticity whithin thermodynamics", Int. J. Solids Struct., 44, 7526-7542, 2007.

[5] H.P. Feigenbaum, Y.F. Dafalias, "Simple model for directional distortional hardening in metal plasticity whithin thermodynamics", J. Eng. Mech., 134, 730-738, 2008.

[6] A.V. Shutov, S. Panhans, and R. Kreissig, "A phenomenological model of finite strain viscoplasticity with distortional hardening", Z. Angew. Math. Mech., 91, 653-680, 2011.

[7] J. Plešek, H.P. Feigenbaum, Y.F. Dafalias, "Convexity of yield surface with directional distortional hardening rules", J. Eng. Mech., 136, 477-484, 2010.

[8] J. Plešek, A. Křístek, "Assessment of methods for locating the point of initial yield", Comp. Meth. Appl. Mech. Engrg., 141, 389-397, 1997.

[9] H.P. Feigenbaum, "Directional distortional hardening in plasticity based on thermodynamics", Ph.D. thesis, UC Davis, USA, 2008.

[10] J. Lemaitre, J.L. Chaboche, "Mechanics of Solid Materials", Cambridge University Press, Cambridge, United Kingdom, 1990.